Magnetic Structures of Rare Earth Metals

Roger A. Cowley
Oxford Physics, Clarendon Laboratory,
Parks Rd, Oxford OX1 3PU, UK
and
Jens Jensen
Ørsted Laboratory, Niels Bohr Institute,
Universitetsparken 5, 2100 Copenhagen, Denmark

Abstract

The recent development in the understanding of the magnetic structures of two rare earth elements are described. These include the observation of distortions in the structures which can only be explained by interactions which break the symmetry between the two superlattices and which have a trigonal form. The observation of a connection between the commensurate modulation, the ordered basal-plane moment and the c/a ratio, and the difference in the magnetic structures of epitaxial grown materials compared with the bulk. The structures of alloys of Ho with non-magnetic Y and Lu and for the alloys of Ho and Er are also reviewed.

1 Introduction

The study of the magnetic structures and interactions in the rare earth metals was one of the topics to which Allan Mackintosh made a major contribution and in which he was most interested. This interest culminated in his book with one of us (Jensen and Mackintosh, 1991) which described in detail both the experimental results and theories of the magnetism of rare earths. In this article our intention is to discuss some of the developments which have taken place since 1991. These developments have arisen even though the basic principles of rare earth magnetism were well established, partly because of the development of new experimental techniques but also because the book provided a stimulus to new work on the rare earth metals. In a short article we cannot discuss the progress made in the whole of rare earth magnetism. We have therefore chosen to concentrate on the magnetic structures of two of the heavy rare earth metals, Ho and Er, of alloys of Ho with the

non-magnetic elements Y and Lu and of alloys of Ho with Er. In the book it was proposed that trigonal interactions may have significant effects on the magnetic structures in these systems. Since then the studies of the long-periodic complex structures in the Ho and Er based materials have confirmed that this is the case.

Nevertheless, there are still some topics which we shall not discuss in detail. One of these is the extensive set of experiments performed particularly with x-ray and neutron scattering techniques to study the properties of the paramagnetic to incommensurately modulated structure by Wang et al. (1991), Gaulin et al. (1988), Thurston et al. (1993, 1994), Lin et al. (1992), Hagen et al. (1992) and Helgesen et al. (1995). Briefly the exponents measured in these experiments are not in agreement with the predictions of any of the theories. Furthermore, the observation of two length scales (Thurston et al., 1993, 1994) in Ho were the first to show that this behaviour occurred in magnetic systems and, although it is now established that the long length scale is associated with the surface, there is still no detailed understanding of the results (Cowley, 1997).

In this paper we shall describe in detail the new results for the low-temperature structures and their implications for the nature of the magnetic interactions. In the next section we describe results and theory for the magnetic structure of holmium and in Sect. 3 similar results for Er. Both of these sets of results demonstrate that the properties of the rare earths cannot be understood solely in terms of single-ion anisotropy and exchange interactions between pairs of spins which depend only quadratically on the spin components. In Sect. 4 we summarise the results obtained on the properties of Ho/Y and Ho/Lu alloys and the information they provide about the magnetic interactions. In Sect. 5 we describe the magnetic structures of Ho/Er alloys and then in a final section summarise the results and outstanding problems.

2 Magnetic structures of holmium

The magnetic structure of Ho was determined initially by Koehler et al. (1966). They showed that between the Néel temperature of 132 K and about 19 K, the magnetic structure consisted of ferromagnetically coupled moments within each basal plane and that the orientation of the moments rotated in successive basal planes giving a helical structure. The average angle of rotation is described by a wavevector $\mathbf{q}$, which has the value of 0.275 $\mathbf{c}^*$ at T_N and reduces on cooling. Below about 19 K the wavevector $\mathbf{q}$ locks in to 1/6 $\mathbf{c}^*$ and the structure develops a ferromagnetic moment along the c axis giving a cone structure. Koehler et al. (1966) and Felcher et al. (1976) showed that the structure was not a homogeneous helix but distorted so as to produce a bunching of the magnetic moments around the easy b axes. The 12-layered commensurable structure in the $1/6\, c^*$ phase consists of

pairs of layers with the moments nearly along the same b axis, while the moments rotate 60° from one pair to the next. The bunching angle between the moments in the pairs and the nearest b axis was found to approach 5.8° in the zero temperature limit.

Gibbs et al. (1985) used x-ray resonant scattering techniques to study Ho and showed that the wavevector did not change smoothly with temperature but that below 30 K there were a series of lock-ins to commensurable structures. They proposed the long-period commensurable structures to be the 12-layered structure modified by regularly spaced spin slips at which only one plane was associated with an easy axis instead of two planes. These spin-slip structures give rise to a characteristic pattern of the neutron scattering which was measured (Cowley and Bates, 1988) and then used to produce detailed models of these structures. These

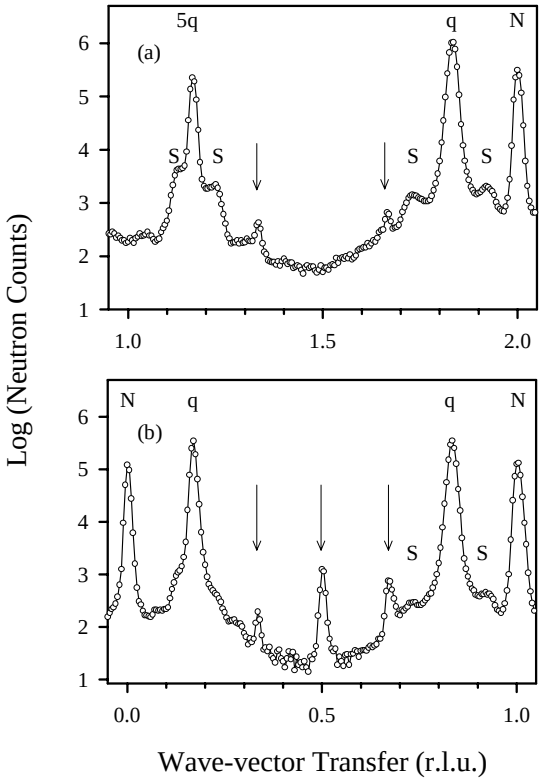

Figure 1. The neutron scattering from Ho at 10 K when the wavevector transfer is varied along (a) [00ℓ] and (b) [10ℓ]. The peaks marked with arrows cannot be accounted for by an undistorted cone structure while the peaks marked S are spurious (Simpson et al., 1995).

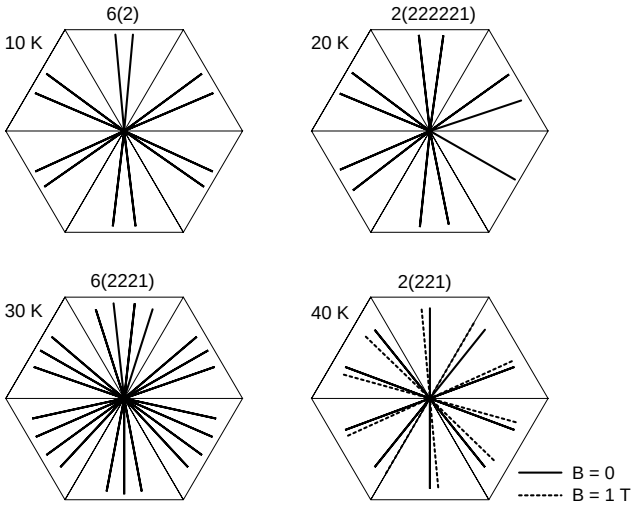

Figure 2. Spin-slip structures in Ho with $\mathbf{q} = 1/6$, 2/11, 4/21, and 1/5 $\mathbf{c}^*$ calculated at 10, 20, 30, and 40 K respectively. The 10-layered structure at 40 K is both calculated at zero field and at a field of 1 T along the c axis.

models compared well with the results obtained later from mean-field calculations (Mackintosh and Jensen, 1991).

Recently Simpson et al. (1995) have performed further neutron scattering studies on Ho to study in particular the structure of the low-temperature cone phase and the transition from it to the basal-plane helix. The results for the scattering observed when the wavevector transfer is varied along $[00\ell]$ and $[10\ell]$ are shown in Fig. 1 at 10 K in the cone phase. The peaks marked N arise from the nuclear setting, the ones marked q from the $q = 1/6\, c^*$ helical structure, the one marked $5q$ from the bunching of the moments around the easy axes, and the weaker ones with arrows are previously unreported peaks with $\mathbf{Q} = (001\frac{1}{3})$, $(001\frac{2}{3})$, $(10\frac{1}{3})$, $(10\frac{1}{2})$ and $(10\frac{2}{3})$. The usually assumed structure of the cone phase cannot account for these peaks as they can only arise if the conventionally assumed symmetry of the cone phase is broken. Figure 2 shows a possible structure which can account for the observations. In the structure shown at 10 K the bunching angle differs for successive easy axes by about 1.3° giving rise to the scattering with $\mathbf{q} = (00\frac{1}{3})$ and the cone tilt angle varies for successive easy axes by about 2.3° giving rise to the $(10\frac{1}{2})$ scattering.

The symmetry breaking arises because the environment of a rare earth atom differs for each of the two sublattices in the hcp structure. Both sublattices have

trigonal, not hexagonal, symmetry, and the trigonal axes are rotated by 60° for one sublattice compared with the other. As pointed out by Jensen and Mackintosh (1991), the lowest order pair-interactions which have this reduced symmetry are of the fourth rank, and one example is:

$$\mathcal{H}_3 = \sum_{ij} \mathcal{K}_{31}^{21}(ij) \left[O_3^2(i) J_y(j) + O_3^{-2}(i) J_x(j) \right], \tag{1}$$

where the Stevens operators are $O_3^{\pm 2} = \frac{1}{2}(J_z O_2^{\pm 2} + O_2^{\pm 2} J_z)$ with $O_2^2 = J_x^2 - J_y^2$ and $O_2^{-2} = J_x J_y + J_y J_x$. The x-, y-, and z-axes are assumed to be along the a-, b-, and c-axes of the hcp lattice, respectively. All of the three fourth-rank terms are similar in that they couple the spin components $J_x^2 J_y J_z$ and $J_y^3 J_z$ but with different components associated with the two sites i and j.

Calculations by Simpson et al. (1995) and by Jensen (1996) using the mean-field model (Larsen et al., 1987) and the data shown in Fig. 1 and other similar results at higher temperatures and in applied magnetic fields, suggests that the largest contribution arises from the $\mathcal{K}_{31}^{21}$ term given by Eq. (1) and that this interaction is about 2% of that of the two-spin exchange interaction.

The effect of the trigonal interaction on the $2/11\,c^*$ commensurate phase was also studied and scattering was observed for $\mathbf{Q} = (0, 0, m/11)$ with m an odd integer. This scattering would be absent if both sublattices had the same symmetry. The contribution of the trigonal coupling to the free energy is of second order in the helical case. The effect is larger for the cone structure, as observed for the $2/11\,c^*$ phase when a c-axis magnetic field of 2 T is applied (Cowley et al., 1991). In the cone phase all three components of the moments have non-zero expectation values leading to a first-order contribution to the free energy which is

$$\Delta F \propto \sum_p (-1)^p J_\parallel J_\perp^3 \cos(3\phi_p). \tag{2}$$

$J_\parallel$ and $J_\perp$ are the components of the magnetic moments parallel and perpendicular to the c axis, respectively, and ϕ_p is the angle the perpendicular component of the moments in the pth layer makes with the x- or a-axis. Thus if only the trigonal anisotropy is important for the cone structure, then every second a axis is an easy axis in one of the sublattices and the other three a axes are the easy axes in the other sublattice.

The experiment of Simpson et al. (1995) also clarified the nature of the lock-in to the cone phase at 19 K. As first noted by Sherrington (1971) there is no reason that the lock-in to $\mathbf{q} = 1/6\ \mathbf{c}^*$ should occur at the same temperature as the c-axis moment develops in the cone phase. Furthermore, specific-heat measurements by Stewart and Collocott (1989) and ultrasonic measurements by Bates et al. (1988) suggested that there might be two transitions. Unfortunately, the measurements

are difficult because of hysteresis, but a study of the temperature dependence of the $(10\frac{1}{3})$ reflections which effectively measure the average cone angle and the $(10\frac{1}{2})$ reflections which measure the existence of the $1/6\,c^*$ phase, showed quite different behaviour and that between 18 K and 19 K the crystal was in a $\mathbf{q} = 1/6\ \mathbf{c}^*$ basal-plane helix with no net ferromagnetic moment, and that below 18 K the crystal underwent a second transition to the cone phase.

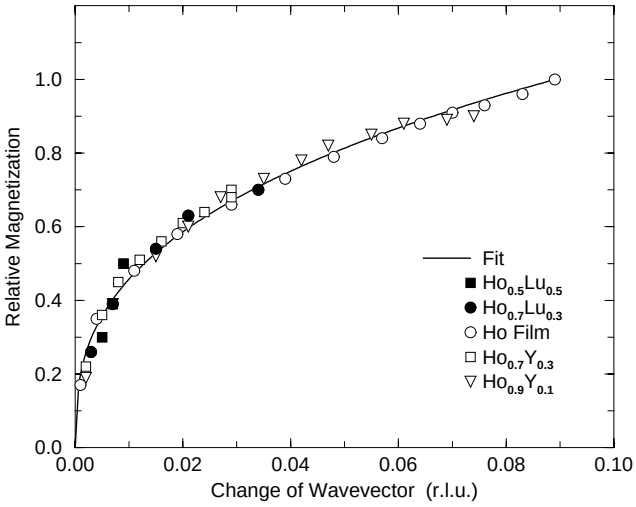

Figure 3. The change in the ordering wavevector of a holmium film, of Ho/Y alloys (Cowley et al., 1994) and of Ho/Lu alloys (Swaddling et al., 1996) as a function of the basal-plane ordered moment.

The variation of the ordering wavevector with temperature has been re-examined by Helgesen et al. (1994) and their results are shown in Fig. 3. Close to T_N the change in the wavevector is proportional to the square of the ordered moment M, as might be expected from the theory of Elliott and Wedgwood (1963), where the change in wavevector results from a change in the position of the superzone gaps at the nesting Fermi-surface. Over much of the temperature range the change in the ordering wavevector is proportional to M^3, but this behaviour is as yet not understood. A further correlation is with the c/a ratio for which Andrianov (1992) discovered that the ordering wavevector was given by

$$q = q_0\big[(c/a)_0 - c/a\big]^{\frac{1}{2}}, \tag{3}$$

where $(c/a)_0$ is 1.582. This result shows that the Fermi-surface properties are strongly correlated with the c/a ratio. Because of these effects any modeling of

the structures by using exchange constants between neighbouring planes must inevitably require temperature-dependent exchange constants.

The mean-field model developed for Ho utilizes the spin-wave measurements at different temperatures to obtain a phenomenological account of the temperature dependence of the exchange coupling. The model has been used for analysing the commensurable effects displayed by the helical ordered basal-plane moments in Ho (Jensen, 1996). At low temperatures the hexagonal anisotropy energy is large and the model predicts strong commensurable effects of the spin-slip structures in consistency with the experiments. Figure 4 shows a comparison between the calculated results and the field experiment of Cowley et al. (1991). The model accounts well for the overall shift of the ordering wavevector with the c-axis field at a constant temperature, and there seems to be no need for invoking a field dependence of the exchange coupling. As shown in Fig. 4 the experiments of Cowley et al. indicated that metastable states appear frequently at low temperatures. They found by measuring the position of the higher harmonics rather than the first harmonic, that the diffraction pattern was determined in many cases by a superposition of neutrons scattered from domains with different commensurable periods.

The hexagonal anisotropy energy decreases very quickly with the magnetisation M, approximately like M^{21}, whereas the change of the trigonal anisotropy energy $\sim M^7$ is more moderate. This means that around 40 K ($M \simeq 0.925 M_0$) the hexagonal anisotropy energy has decreased by a factor of 5 whereas the trigonal anisotropy is only reduced by a factor of 1.7, compared with the zero-temperature values. The trigonal contribution is strongly enhanced by a c-axis field, Eq. (2). In combination the two effects imply that although the trigonal distortions of the helix at 40 K are small at zero field, they dominate in a c-axis field of 1 T. At this field the 10-layered structure is predicted to be the one shown in Fig. 2, where the moments in the two spin-slip layers are oriented along an a axis instead of a b axis as at zero field. This modification leads to a strong increase of the commensurability of the 10-layered structure. At zero field the model indicates that this structure is stable within a temperature interval around 42 K of about 2.2 K, which increases to about 10 K at a c-axis field of 1 T, whereupon the lock-in interval stays more or less constant between 1 and 5 T. The hysteresis effects detected by Cowley et al. (1991) below 35 K may possibly explain why the lock-in intervals determined by Tindall et al. (1993) are somewhat smaller than predicted by the theory. They only studied the behaviour of the first harmonic which did not indicate any lock-in at zero field, and at 3 T the lock-in interval was found to be 2–3 K.

Around 100 K the spin-slip model no longer applies. The hexagonal anisotropy only manages to rotate the moments by about one tenth of a degree. At this temperature the ordering wavevector is close to $1/4\, c^*$, but the model indicates only a marginal lock-in to the 8-layered structure. In the presence of a c-axis field of 3 T,

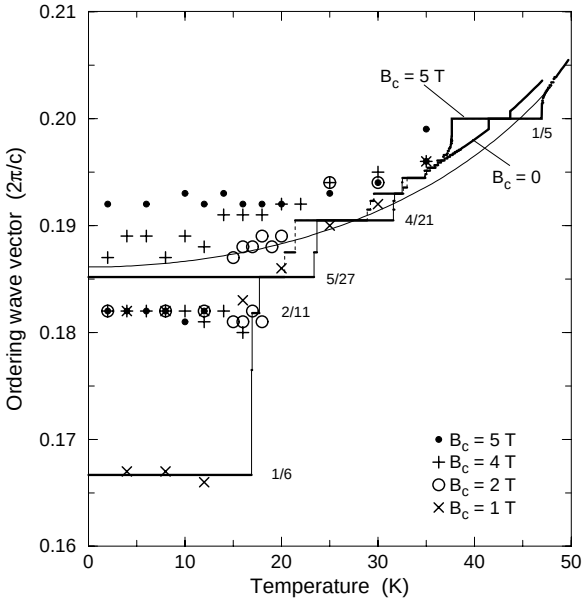

Figure 4. The ordering wavevector in Ho. The calculated results are shown by the horizontal solid lines connected with vertical thin solid or thin dashed lines corresponding respectively to the results obtained at zero or at a field of 5 T applied along the c axis. The symbols show the experimental results of Cowley et al. (1991) obtained at the various values of the c-axis field defined in the figure. The smooth curve shown by the thin solid line is the temperature dependent position of the maximum in the exchange coupling assumed in the model.

the trigonal coupling increases the bunching effect by a factor of 4, but the lock-in interval is still estimated to be very small, about 0.1 K. In analogy with the fifth and seventh harmonics induced by the hexagonal anisotropy, the first-order term in the free energy due to the trigonal coupling induces a second and a fourth harmonic. Because of the factor $(-1)^p$ in Eq. (2) these harmonics are translated a reciprocal lattice vector along the c axis (half of a reciprocal lattice vector in the double-zone scheme), which means that the fourth harmonic appears at zero wavevector when $\mathbf{q} = 1/4\ \mathbf{c}^*$. In other words, in the case of a cone structure with a period of 8 layers the trigonal coupling leads to a ferromagnetic component perpendicular to the c axis. Although it is small, this component has a determining effect in forming the commensurable structure. The lock-in interval increases proportionally to $\sqrt{\theta}$, where θ is the angle the field makes with the c axis, and even the slightest deviation

of the field from perfect alignment along the c axis will produce a sizable lock-in effect. The lock-in interval is calculated to be 2.7 K at $\theta = 1°$ at the field of 3 T. Both this value and the very weak lock-in effect at zero field are consistent with the observations (Noakes et al., 1990; Tindall et al., 1991). In the experiments the field was applied nominally along the c axis but with an uncertainty of about 2° corresponding to an effective $\theta \simeq 1°$. At a larger tilt angle of the field the lock-in interval is estimated to increase up to a value of 8–12 K.

The increased stability of the 10-layered periodic structure around 42 K and of the 8-layered one around 96 K, observed when applying a field along the c axis can not be explained without the trigonal anisotropy term. If this term is neglected the anisotropy effects and therefore also the commensurable effects on the helical structures, decrease rapidly with a field applied in the c-direction (misalignment effects are estimated to be unimportant in this situation). The model including the trigonal interactions explains most of the commensurable effects observed in Ho except for the lock-in of the $5/18\,c^*$-structure observed in an interval of 5 K just below T_N in a b-axis field of 3 T (Tindall et al., 1994). The model only predicts a marginal lock-in in this case, which discrepancy is most likely a consequence of the limited validity of the mean-field approximation in this close neighbourhood of the phase transition.

One further set of measurements on the magnetic properties of holmium has been the result of the growth of Ho films grown by molecular beam epitaxy. Usually the films have been grown by the techniques developed by Kwo et al. (1985) in which a Nb film is deposited on a sapphire substrate, to provide a chemical buffer and then a seed layer of a non-magnetic material such as Y or Lu is deposited. The holmium is then grown to the appropriate thickness with the c axis as the growth direction and the samples are capped with Y or Lu to prevent oxidation of the holmium layer. This procedure typically leads to samples with a mosaic spread of about 0.15°. The films are single crystals and the basal-plane lattice constants are different from those of the seed layer or capping layer and very similar to those of the lattice constant of bulk holmium above T_N.

The magnetic structures have been determined for Ho films grown on Y (Jehan et al., 1993; Swaddling, 1995), Lu (Swaddling, 1995) and Sc (Bryn-Jacobsen et al., 1997). In the case of Y films of thickness 1500 Å, 5000 Å, and 15000 Å have been studied, while for a Lu seed the thickness was 5000 Å and for the Sc seed, 2500 Å. The wavevector for the onset of ordering was the same as for bulk holmium but, the wavevector at low temperature was in some cases larger than that of the bulk: $1/5\,c^*$ and $5/27\,c^*$ for the 15000 Å film on Y, $1/5\,c^*$ and $4/21\,c^*$ for the 5000 Å film on Y, $1/6\,c^*$ and $7/39\,c^*$ for the 5000 Å film on Lu and $7/39\,c^*$ for the 2500 Å film on Sc. The results for the films on Y show that there is little change in wavevector with film thickness for these thick films. There is a change in the

behaviour with substrate and hence strain but that all the films have on average larger wavevectors than the bulk even though for the Y seeds, the basal planes of the Ho are expanded while for the Sc and Lu seed layers, they are compressed. In all the films the ferromagnetic cone phase is suppressed except for the 15000 Å film for which the c-axis moment is much less than for the bulk. These results and the differences from the bulk behaviour are not understood in detail but presumably arise from the clamping of the basal-plane lattice parameter of the films.

3 Magnetic structures of erbium

The crystal-field interactions in erbium are of opposite sign to those of holmium so that the structures have a c axis or longitudinal component to the magnetic ordering. The magnetic structures were determined by Cable et al. (1965) as

(i) between $T_N = 84$ K and $T'_N = 52$ K, a roughly sinusoidal variation of the longitudinal component of the magnetisation with a wavevector of about $\mathbf{q} = 0.277$ $\mathbf{c}^*$.

(ii) between T'_N and $T_C = 18$ K the wavevector decreases to $\mathbf{q} = 0.25$ $\mathbf{c}^*$ and transverse basal-plane components of the moments are ordered with the same wavevector as the longitudinal ones.

(iii) below T_C the magnetic structure is a cone with a basal-plane modulation of $\mathbf{q} = 5/21$ $\mathbf{c}^*$ and a ferromagnetic c-axis component.

Subsequent measurements by Habenschuss et al. (1974) showed that the structures were distorted from the simple ones. High-resolution x-ray scattering measurements by Gibbs et al. (1986) showed that in phase (ii) the wavevector locked into a series of commensurate wavevectors with $\mathbf{q} = 1/4$, $6/23$, $5/19$ and $4/15$ $\mathbf{c}^*$ and proposed that these structures resulted from there being either 4 or 3 successive basal-planes having their moments along the positive or negative c axis.

More recently high-resolution neutron scattering measurements have been performed to study these phases in more detail (Cowley and Jensen, 1992). Measurements were made of the higher harmonics and the results interpreted to deduce the structures. The results shown in Fig. 5 were obtained for the $\mathbf{q} = 4/15$ $\mathbf{c}^*$ phase at 35 K and show a large number of higher harmonics. Initially the data showed that phase (ii) could be described approximately as a cycloidal structure in which the moments rotate in an a–c plane. Nevertheless this structure cannot describe the data shown in Fig. 5 because, if both sublattices are identical, the peaks with $\mathbf{Q} = (0, 0, n/15)$ with n odd should be absent and although they are weak, their intensity is clearly non-zero. The origin of these peaks is distortions of the structure arising from the trigonal terms already discussed in Sect. 2. The structure is not a planar cycloid in the a–c plane but a wobbling cycloid in

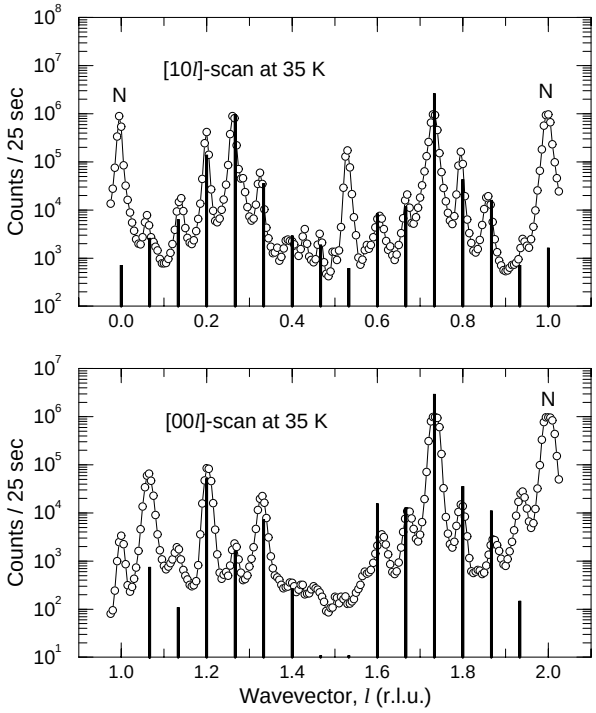

Figure 5. Neutron scattering from Er at 35 K. The upper part shows the results obtained when the wavevector transfer was scanned along $[10\ell]$ and along $[00\ell]$ in the lower figure. The peaks marked N are from nuclear scattering and the others are magnetic scattering. The wavevector of the cycloidal phase is $\mathbf{q} = 4/15\ \mathbf{c}^*$. The thick vertical lines are the intensities predicted by the mean-field calculations including the trigonal interactions. The experimental data have not been corrected for extinction or spurious scattering effects (Cowley and Jensen, 1992).

which the structure has deviations away from the plane (Cowley and Jensen, 1992; Jensen and Cowley, 1993). A mean-field calculation and a careful comparison with the experimental results suggested that the dominant trigonal term was $\mathcal{K}_{31}^{21}$ as also found for holmium, Sect. 2, and that the interaction is about 15% of the two-spin exchange interaction. The agreement for the $4/15\,c^*$ phase between the observed scattering and that calculated by the model is illustrated schematically in Fig. 5. Similar results were obtained for five other commensurable structures in the intermediate phase and for the cone structure below T_C (Cowley and Jensen, 1992). The trigonal interactions are also possibly responsible for the lock-in of the cone phase to $\mathbf{q} = 5/21\ \mathbf{c}^*$. In erbium the cone angle is small so that the basal-plane anisotropy makes only a small contribution to the energy and it is more likely that the lock-in energy arises from the trigonal interactions.

There is also still some uncertainty about the behaviour of Er between T_N and T'_N. In principle, there is the possibility of the longitudinal and transverse moments ordering at different temperatures and, if the exchange is anisotropic, at different wavevectors. Since the single-ion anisotropy favours the longitudinal ordering this ordering occurs at the higher temperature T_N, and the basal-plane components might then order at a lower temperature. As the moments increase entropy effects would then cause a lock-in between the longitudinal and transverse components into a cycloidal phase. Experimentally there is some suggestion that above T'_N but below T_N the basal-plane components show short-range order into a helical structure with a slightly different wavevector from the longitudinal components. This indicates that the transverse moments may be close to order at the different wavevector just above the transition to the cycloidal phase, and thus that the exchange coupling is anisotropic. The intensities are, however, very small and further work is needed to confirm these results.

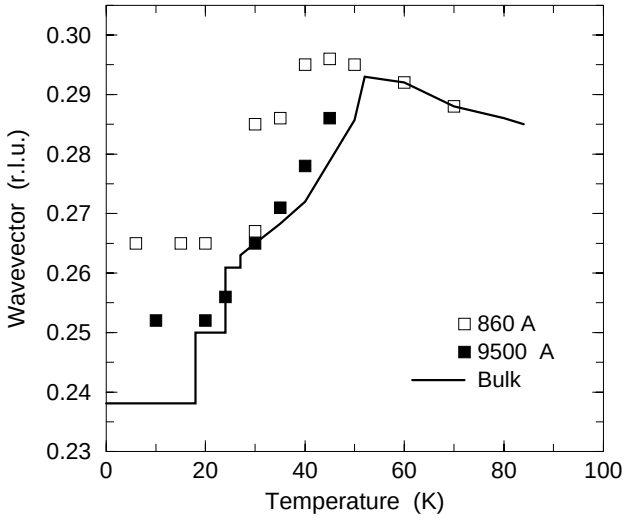

Figure 6. The temperature dependence of the ordering wavevector for bulk Er and for 860 and 9500 Å thick Er films (Borchers et al., 1994).

The ordering wavevector for bulk Er is shown as a function of temperature in Fig. 6 (Gibbs et al., 1986). It differs from that of bulk Ho in that in the longitudinal phase, the wavevector increases with decreasing temperature. This increase is characteristic also of Tm which has a longitudinally modulated phase. Once the basal-plane components order below T'_N, the wavevector decreases with

decreasing temperature as found for Ho. This shows that the decrease is most strongly correlated with the basal-plane component of the magnetic ordering. The same is valid though to a lesser extent also for the changing of the c/a ratio.

Er thin films grown on a Y seed have been studied by Borchers et al. (1991a, 1991b). They studied films with thicknesses between 375 Å and 14000 Å and found that T_N only slightly decreased as the film thickness decreased. In all the films the structure was a longitudinally modulated structure below T_N and there was an ordering of the basal-plane components below about 45 K. In Fig. 6 we show the measured wavevectors for the moments in a 9500 Å thick film, and the results are very similar to those of bulk Er except for the suppression of the cone phase. The results for the thinner films are similar except that the wavevectors tend to lie above those of bulk Er and that the low-temperature structures are commensurate phases with $\mathbf{q} = 5/19$ or $4/15\ \mathbf{c}^*$. The suppression of the cone phase is presumably, as for Ho films, due to the clamping of the basal planes by the substrate and seed layers.

4 The magnetic properties of Ho-Y and Ho-Lu alloys

One of the advantages of the development of artificial growth facilities like molecular beam epitaxy, is that it enables the growth of high quality uniform alloy samples. The samples are grown in the same manner as described for the Ho films in Sect. 2 but with the sample being produced by using the fluxes from two sources controlled so as to produce a constant composition alloy. Using these techniques, measurements have now been made of Ho/Y alloys (Cowley et al., 1994), Ho/Lu alloys (Swaddling et al., 1996) and Ho/Sc alloys (Bryn-Jacobsen et al., 1997). Earlier experiments on bulk powdered alloy samples were performed by Child et al. (1965). The results of measurements on single-crystal films and on powdered bulk samples are in general agreement with one another but the accuracy obtainable with powdered samples is not sufficient to test this in detail. In all the cases the thin-film samples have mosaic spreads of about 0.15°.

For all of the samples, the magnetic structures are found to be basal-plane helices with a wavevector dependence as illustrated in Fig. 7 for Ho/Y alloys. The wavevector for the onset of magnetic ordering is independent of concentration and decreases with decreasing temperature but by amounts which decrease with increasing Y concentration. The results for the Ho/Lu alloys are also shown in Fig. 7, and the behaviour is qualitatively similar but differs in that the wavevector for the onset of magnetic order decreases as the Lu concentration increases. Figure 8 shows the behaviour of T_N as a function of Ho concentration. These results can be compared

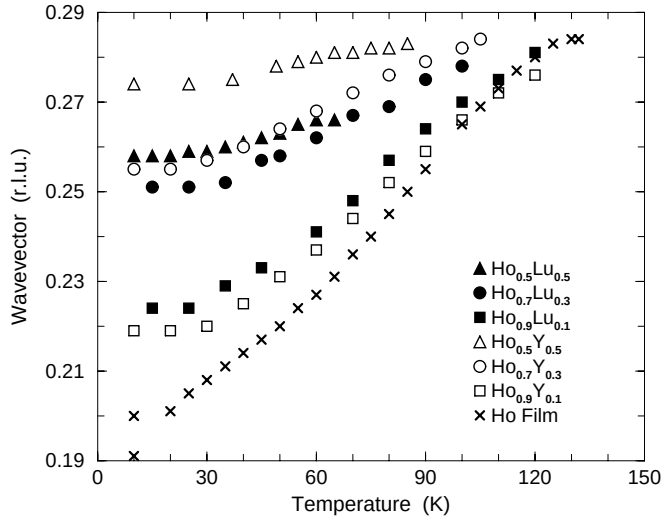

Figure 7. The wavevector for the basal-plane ordering of Ho/Y and of Ho/Lu alloys as a function of temperature and compared with a similar Ho film (Swaddling et al., 1996; Cowley et al., 1994).

with those of Child et al. (1965) for a range of bulk alloy systems which suggested that T_N was a universal function of the de Gennes factor $x = c(g-1)^2 J(J+1)$ and that T_N was proportional to $x^{2/3}$. This empirical result has little theoretical basis because mean-field theory suggests that T_N is proportional to x and even then the theory would only be valid if the conduction-electron susceptibility of all rare earth metals was the same. Although this result is successful at describing the overall trends, it cannot be expected to describe the detailed behaviour of particular systems and indeed, as shown in Fig. 8, fails for Ho/Lu alloys and to a lesser extent for Ho/Y alloys.

A more reasonable description of the alloys is to assume an average or virtual crystal model of the conduction-electron susceptibility when

$$T_N(c) = c\big[cT_{\mathrm{Ho}} + (1-c)T_\gamma\big], \tag{4}$$

where T_γ is T_N for bulk Ho if it had the conduction-electron susceptibility of the alloying element γ. As shown in Fig. 8, Eq. (4) provides a good description of the results with $T_{\mathrm{Ho}} = 132 \pm 2$ K, $T_{\mathrm{Y}} = 207 \pm 3$ K and $T_{\mathrm{Lu}} = 144 \pm 2$ K. This then suggests that the peak in the conduction-electron susceptibility for Y is 1.64 times larger than for Ho while that for Lu is 1.09 times larger. It is similarly possible to

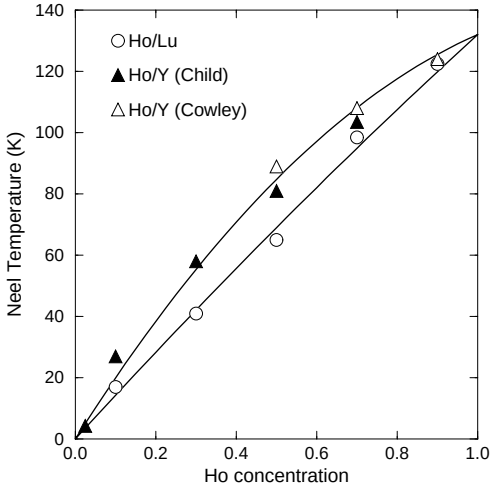

Figure 8. The dependence of T_N on concentration for Ho/Y and Ho/Lu alloys (Swaddling et al., 1996).

extrapolate the wavevector for the onset of magnetic order to give the wavevector for the peak of the susceptibility for Ho as 0.282 ± 0.004 **c***, Y as 0.282 ± 0.004 **c*** and Lu as 0.235 ± 0.015 **c***. This analysis assumes an average crystal model and neglects critical fluctuations, but its success suggests that there is considerable validity in the approach.

Figure 3 of Sect. 2 shows that the change in wavevector with temperature is correlated with the ordered moment in Ho. The figure also shows a similar relationship for Ho/Lu and Ho/Lu alloys, and that $\Delta q \sim M^{\alpha}$ with $\alpha = 2.8 \pm 0.3$ from a combined fit to all of the results.

At low temperatures all of the alloy samples lock-in to commensurate structures: $\mathbf{q} = 2/9$ **c*** for $c = 0.9$, $\mathbf{q} = 1/4$ **c*** for $c = 0.7$, $\mathbf{q} = 8/31$ **c*** for $c = 0.5$ in Ho/Lu alloys and $\mathbf{q} = 3/11$ **c*** for Ho/Y alloys. Clearly, therefore, the concepts developed for the bulk rare earth materials can be taken over to the alloy systems. Of particular interest is the phase diagram of the Ho/Y alloy with $c = 0.7$ in an applied basal-plane field which shows not only the low-field helical phase and a high field fan phase but between these phases at low temperatures an exceptional clear example of a helifan phase (Jensen and Mackintosh, 1990; Mackintosh and Jensen, 1991, 1992) which is stable over a considerable range of parameters.

5 The magnetic structure of Ho/Er alloys

Ho/Er alloys are of interest because of the competing anisotropy of the Ho and Er atoms. The first experiments on this system were by Pengra et al. (1994) who studied a bulk crystal with $c = 0.5$. The experiments reported below (Simpson et al., 1997) were obtained by studying thin-film alloy samples grown as described in Sect. 2 and the results obtained are different from those obtained on bulk samples. Further work is needed to find out the reasons for these differences.

Three alloy systems have been studied as thin films of Ho_cEr_{1-c} with $c = 0.8$, 0.5 and 0.3. In all cases the neutron scattering intensity was measured along $[00\ell]$ to determine the basal-plane ordering, and along $[10\ell]$ to determine the longitudinal ordering. No evidence was found of scattering from higher harmonics suggesting that the moments are ordered in a largely sinusoidal pattern.

For $c = 0.8$, the ordering wavevector decreases with decreasing temperature until it locks in to $\mathbf{q} = 1/5\ \mathbf{c}^*$ below 20 K. The magnetic structure is a basal-plane spiral until surprisingly below 20 K the moment tilts out of the plane to form a cone phase with a cone angle of $75° \pm 2°$. This is unexpected because films of Ho, Ho/Y and Ho/Lu alloys have not shown cone phases. Preliminary measurements on bulk crystals of Ho_cEr_{1-c} with $c = 0.9$ and 0.5 indicates that T_C is higher in the alloy systems than in either Ho or Er, and this is found to be in accord with mean-field predictions (Rønnow, 1996). The opposite signs of the single-ion axial anisotropy in Ho and in Er imply that the average or effective axial anisotropy changes its sign at a higher temperature in the alloy systems than in pure Ho.

The behaviour of the sample with $c = 0.5$ is more complex. The basal-plane moments order below 110 ± 2 K with a wavevector $\mathbf{q} = 0.282\ \mathbf{c}^*$. The wavevector then reduces steadily with decreasing temperature with the possibility of lock-ins to structures with $\mathbf{q} = 8/31\ \mathbf{c}^*$, $1/4\ \mathbf{c}^*$, $8/33\ \mathbf{c}^*$, and $3/13\ \mathbf{c}^*$. The structure is a basal-plane spiral above 50 K and then becomes at least partially a cycloid until 30 K when the structure becomes a cone phase with a cone angle of 67° at 20 K.

The third sample with $c = 0.3$ developed magnetic order as a basal-plane helix with $\mathbf{q} = 0.288\ \mathbf{c}^*$ at $T_N = 94 \pm 2$ K. The structure remained a basal-plane helix down to 80 K while the wavevector reduced. On further cooling there was ordering in the longitudinal moments and the structure developed a cycloidal phase below 60 K. Between 35 K and 22 K the magnetic structure was a $\mathbf{q} = 1/4\ \mathbf{c}^*$ cycloidal phase, and below 22 K the wavevector became $\mathbf{q} = 5/21\ \mathbf{c}^*$ and the structure became a cone with a cone angle of $44° \pm 5°$.

These results are summarised in the schematic phase diagram in Fig. 9. The unexpected feature is that in all the systems the low-temperature phase is a cone phase unlike thin films of Er or Ho, Sects. 2 and 3. The basal-plane helical ordering presumably of the Ho moments dominates at temperatures above T_N of bulk

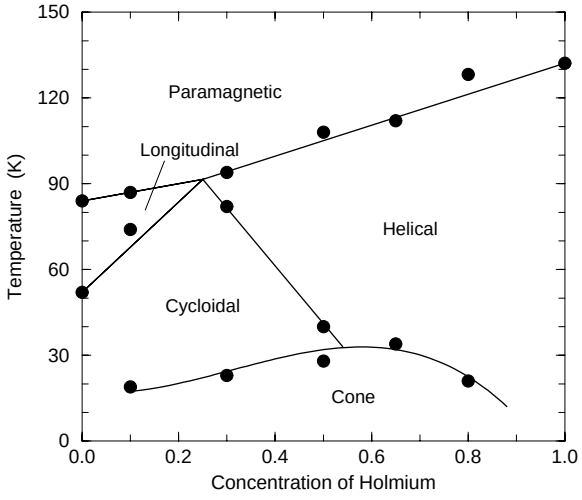

Figure 9. A schematic phase diagram for thin films of Ho/Er alloys deduced from the measurements of Simpson et al. (1997).

erbium. On cooling for larger concentrations of Er the structure becomes a cycloid with the possibility of commensurate phases similar to those of Er before forming a cone phase at low temperature. This behaviour is at least qualitatively consistent with the approximate cancellation of the axial and basal-plane crystal-field anisotropy in Ho/Er alloys with $c = 0.5$.

6 Summary and Conclusions

The results described in the previous sections show that there have been considerable developments in our understanding of the rare earth metals particularly on the experimental side. The strongest magnetic interactions are the well known single-ion crystal fields and the exchange interactions conveyed through the conduction electrons. Nevertheless, there are now many experiments (Sects. 2 and 3) which show that some important aspects also require there to be trigonal interactions between sites. These terms must arise from the effect of the spin-orbit interactions on the conduction electrons, but there is as yet no quantitative understanding.

The ferromagnetic structures (Gd and the low-temperature phases in Tb and Dy) or the longitudinally polarized c-axis modulated structures (Tm and Er between T_N and T_N') are not affected by the trigonal coupling. Therefore the only remaining candidates among the elemental heavy rare earths to be investigated for

the possible structural effects of the trigonal coupling, are Tb and Dy in their high-temperature helical phases. Of these two only Dy may be a realistic possibility, because the helical phase in Tb only occurs in a narrow temperature range.

Ho and Er and their alloys are found to have commensurate locked-in structures not only at low temperatures, but, in Ho, even very close to T_N. Except for the lock-in of Ho close to T_N at $\mathbf{q} = 5/18\,\mathbf{c}^*$ in a b-axis field, the mechanisms behind the commensurable effects are now well understood. The lock-in temperature interval of the $1/5\,c^*$ phase in Ho is predicted to be larger than indicated by the variation in the position of the first harmonic, and a study of the behaviour of the fifth or seventh harmonics will be useful for a clarification of the experimental situation. The strong lock-in of the 8-layered structure in Ho around 96 K indicated by the mean-field model, deserves further studies in which the field is applied by purpose in a direction making a non-zero angle with the c axis or with the basal plane.

The neutron diffraction experiments show that Ho may contain several domains with different commensurable structures below 40 K. In this spin-slip regime there is also the possibility that the positions of the spin-slip layers in the different domains are disordered to some extent. The x-ray experiments (Helgesen at al., 1990, 1992) indicate that this is the case by showing a reduction of the longitudinal correlation length between 40 and 20 K by a factor of 3, a reduction which is partly removed when the spin-slip layers disappear at the lock-in to the 12-layered structure at about 20 K. In the alloy $Ho_{0.9}Er_{0.1}$ the $7/36\,c^*$ structure is stable at the lowest temperatures, and Rønnow (1996) has observed that the widths of the neutron diffraction peaks in this phase are much larger for the higher harmonics than for the first one. The $7/36\,c^*$ spin-slip structure consists of alternating two and three pairs of layers between the spin-slip planes, (2212221), and Rønnow has found that a structure in which the succession of the two sequences is completely random, predicts a diffraction spectrum close to the observed one. Hence the large hexagonal anisotropy in Ho at low temperatures strongly resists a rotation of the moments from one easy direction to the next and may cause a spin-glass like situation.

It is now also empirically known that there is a strong correlation between the ordering wavevector, the c/a ratio and the ordered moment but as yet there is no theory of this connection. Maybe now, with the increasing computer power, is the time for a more realistic calculation of $\mathcal{J}(\mathbf{q})$ mediated by the conduction electrons in the rare earths and for the changes in $\mathcal{J}(\mathbf{q})$ on ordering, using realistic wavefunctions rather than the free electron model of Elliott and Wedgwood (1963). There is a steadily increasing amount of experimental information which could be compared with such calculations.

Finally, there has been much recent interest in artificially grown thin films, alloys and superlattices. The experiments on the alloys have led to a better knowledge of the conduction-electron susceptibilities in Y and Lu, and to a better knowledge of

the phase diagrams and the effects of competing interactions. As yet there has not been much theoretical work performed with which these results can be compared.

Acknowledgements

We are indebted to Allan Mackintosh for his help and inspiration with our work on rare earths. We are grateful to our collaborators: C. Bryn-Jacobsen, K.N. Clausen, D.A. Jehan, D.F. McMorrow, H.M. Rønnow, J.A. Simpson, P. Swaddling, R.C.C. Ward and M.R. Wells. EPSRC has provided financial support in Oxford and the EU LIP programme for support for the experiments at Risø.

References

Andrianov AV, 1992: JETP Lett. **55**, 666

Bates S, Patterson C, McIntyre GJ, Palmer SB, Mayer A, Cowley RA and Melville R, 1988: J. Phys. C **21**, 4125

Borchers JA, Salamon MB, Erwin RW, Rhyne JJ, Du RR, and Flynn CP, 1991a: Phys. Rev. B **43**, 3123

Borchers JA, Salamon MB, Erwin RW, Rhyne JJ, Nieuwenhuys GJ, Du RR, Flynn CP and Beach RS, 1991b: Phys. Rev. B **44**, 11814

Bryn-Jacobsen C, Goff J, Cowley RA, McMorrow DF, Wells MR and Ward RCC, 1997: (to be published)

Cable JW, Wollan EO, Koehler WC and Wilkinson MK: 1965, Phys. Rev. **140**, A 1896

Child HR, Koehler WC, Wollan EO and Cable JW, 1965: Phys. Rev. **138**, A 1655

Cowley RA, 1997: Proc. of 15th Conference on Condensed Matter of the European Physical Society, Physica Scripta, (to be published)

Cowley RA and Bates S, 1988: J. Phys. C **21**, 4113

Cowley RA and Jensen J, 1992: J. Phys. Condens. Matter **4**, 9673

Cowley RA, Jehan DA, McMorrow DF and McIntyre GJ, 1991: Phys. Rev. Lett. **66**, 1521

Cowley RA, Ward RCC, Wells MR, Matsuda M and Sternlieb B, 1994: J. Phys. Condens. Matter **6**, 2985

Elliott RJ and Wedgwood FA, 1963: Proc. Phys. Soc. **81**, 846

Felcher GP, Lander GH, Ari T, Sinha SK and Spedding FH, 1976: Phys. Rev. B **13**, 3034

Gaulin BD, Hagen M and Child HR, 1988: J. Phys. (Paris) Coll. **49**, C8-327

Gibbs D, Moncton DE, D'Amico KL, Bohr J and Grier BH, 1985: Phys. Rev. Lett. **55**, 234

Gibbs D, Bohr J, Axe JD, Moncton CE and D'Amico KL, 1986: Phys. Rev. B **34**, 8182

Habenschuss M, Stassis C, Sinha SK, Deckman HW and Spedding FH, 1974: Phys. Rev. B **10**, 1020

Hagen M, Child HR, Fernandez-Baca JA and Zaretsky JL, 1992: J. Phys. Condens. Matter **4**, 8879

Helgesen G, Hill JP, Thurston TR, Gibbs D, Kwo J and Hong M, 1994: Phys. Rev. B **50**, 2990

Helgesen G, Hill JP, Thurston TR and Gibbs D, 1995: Phys. Rev. B **52**, 9446

Jehan DA, McMorrow DF, Cowley RA, Ward RCC, Wells MR, Hagmann N and Clausen KN, 1993: Phys. Rev. B **48**, 5594

Jensen J, 1996: Phys. Rev. B **54**, 4021

Jensen J and Cowley RA, 1993: Europhys. Lett. **21**, 705

Jensen J and Mackintosh AR, 1990: Phys. Rev. Lett. **64**, 2699
Jensen J and Mackintosh AR, 1991: *Rare Earth Magnetism: Structures and Excitations* (Oxford University Press, Oxford)
Koehler WC, Cable JW, Wilkinson MK and Wollan EO, 1966, Phys. Rev. **151**, 414
Kwo J, Gyorgy EM, McWhan DB, DiSalvo FJ, Vettier C and Bower JE, 1985: Phys. Rev. Lett. **55**, 1402
Larsen CC, Jensen J and Mackintosh AR, 1987: Phys. Rev. Lett. **59**, 712
Lin H, Collins MF, Holden TM and Wei W, 1992: Phys. Rev. B **45**, 12873
Mackintosh AR and Jensen J, 1991: in *Disorder in Condensed Matter Physics*, eds. J.A. Blackman and J. Taguena (Clarendon Press, Oxford) p. 213
Mackintosh AR and Jensen J, 1992: Physica B **180&181**, 1
Noakes DR, Tindall DA, Steinitz MO and Ali J, 1990: J. Appl. Phys. **67**, 5274
Pengra DB, Thoft NB, Wulff M, Feidenhansl R and Bohr J, 1994: J. Phys. Condens. Matter **6**, 2489
Rønnow HM, 1996: *Magnetic Properties of Holmium–Erbium Alloys*, Thesis (University of Copenhagen)
Sherrington D, 1971: Phys. Rev. Lett. **28**, 364
Simpson JA, McMorrow DF, Cowley RA and Jehan DA, 1995: Phys. Rev. B **51**, 16073
Simpson JA, McMorrow DF, Cowley RA, Ward RCC and Wells MR, 1997: (to be published)
Stewart AM and Collocott SJ, 1989: J. Phys. Condens. Matter **1**, 677
Swaddling PP, 1995: *The Chemical and Magnetic Structure of Rare Earth Superlattices and Thin Films*, Ph.D. thesis (University of Oxford)
Swaddling PP, Cowley RA, Ward RCC, Wells MR and McMorrow DF, 1996: Phys. Rev. B **53**, 6488
Thurston TR, Helegesen G, Gibbs D, Hill JP, Gaulin BD and Shirane G, 1993: Phys. Rev. Lett. **70**, 3151
Thurston TR, Helegesen G, Hill JP, Gaulin BD and Simpson PJ, 1994: Phys. Rev. B **49**, 15730
Tindall DA, Adams CP, Steinitz MO and Holden TM, 1994: J. Appl. Phys. **75**, 6318
Tindall DA, Stenitz MO and Holden TM, 1993: Phys. Rev. B **47**, 5463
Tindall DA, Stenitz MO, Kahrizi M, Noakes DR and Ali N, 1991: J. Appl. Phys. **69**, 5691
Wang J, Belanger DP and Gaulin BD, 1991: Phys. Rev. Lett. **66**, 3195